Al nanocluster arrays on Si(111)-7×7 surfaces: Formation process and interactions among clusters

Run-Wei Li,[1,*] Hongjun Liu,[3,4] J. H. G. Owen,[1] Y. Wakayama,[2] K. Miki,[3,4] and H. W. Yeom[5]
[1]*International Center for Young Scientists (ICYS), National Institute for Materials Science (NIMS), 1-1 Namiki, Tsukuba, Ibaraki 305-0044, Japan*
[2]*Advanced Electronic Materials Center, National Institute for Materials Science (NIMS), 1-1 Namiki, Tsukuba, Ibaraki 305-0044, Japan and Nanoscale Quantum Conductor Array Project, ICORP, JST, Japan*
[3]*Organic Nanomaterials Center, National Institute for Materials Science (NIMS), 1-1 Namiki, Tsukuba, Ibaraki 305-0044, Japan*
[4]*Graduate School of Pure and Applied Sciences, University of Tsukuba, Tsukuba, Ibaraki 305-0005, Japan*
[5]*Center for Atomic Wires and Layers and Institute of Physics and Applied Physics, Yonsei University, Seoul 120-749, Korea*
(Received 2 November 2006; revised manuscript received 6 May 2007; published 15 August 2007)

By means of variable-temperature scanning tunneling microscopy, we have investigated systematically the formation process of Al magic cluster arrays on the Si(111)-7×7 surface at high temperature in situ. It was found that the magic clusters form only when the Al coverage is over a critical value, ~0.08±0.015 ML. These clusters occupy preferentially on the faulted-half-unit cells of the Si(111)-7×7 surface, but this preference is coverage dependent. By analyzing systematically the spatial distribution of magic clusters below the saturation coverage, an attractive interaction between clusters was found, which prevents a triangular ordering of the nanocluster array.

DOI: 10.1103/PhysRevB.76.075418 PACS number(s): 81.16.Dn, 61.46.Bc, 68.18.Jk

I. INTRODUCTION

Due to potential applications in nanocatalysis, nanoelectronics, optical devices, quantum computing, and cryptography,[1–8] the fabrication of large-scale and highly ordered metal nanocluster arrays on solid substrates has been an intensively pursued topic. Particularly, with the aim of integrating nascent spintonic and molecule electronic devices into conventional electronics built on the conventional semiconductor Si, the fabrication and characterization of highly ordered functionalized nanostructures on Si surfaces have attracted extensive efforts. Recently, identically sized ("magic") cluster arrays[9–16] have been fabricated on Si(111) surfaces for various metal elements. For example, Tl (Ref. 9) and In (Ref. 11) magic clusters are formed and occupy only the faulted-half-unit cells (FHUCs) of the Si(111)-7×7 surface at the initial stage; as a result, a large-scale two-dimensional (2D) triangular cluster array (a so-called nanocluster crystal) is formed on the Si(111)-7×7 template. For the case of Ga,[11] as well as Al,[12,13] nanoclusters are formed within both FHUCs and unfaulted-half-unit cells (UHUCs) and self-organize into a nanocluster array with a honeycomb structure. Such arrays could possibly be used as a perfect artificial interface or template for fabricating functionalized large-scale metal/alloy cluster arrays or single molecule arrays.

An atomic structure model for magic metal nanoclusters on the Si(111)-7×7 surface has been proposed theoretically based on scanning tunneling microscopy (STM) observations.[12,13,16] For example, in the case of magic Al nanoclusters, each Al nanocluster consists of six Al adatoms and three Si center adatoms which are displaced toward the center of the Si(111)-7×7 half unit cell. However, the driving force for the formation of magic nanoclusters and their arrays with a nearly perfect periodic structure remains unclear as yet although this is very important for understanding the underlying self-organization process.

In our previous studies,[17,18] the dynamic behavior of Al magic clusters on the Si(111)-7×7 surface at high temperature has been investigated by variable-temperature STM. It was found that fast diffusion of magic Al clusters occurs above 500 °C, with an activation energy of 2.0±0.3 eV, together with the decomposition of the clusters into the $\sqrt{3} \times \sqrt{3}$-Al phase. In this work, we present further in situ STM observations on the formation process of Al nanoclusters and their arrays on the Si(111)-7×7 surface at high temperature. It was found that Al magic clusters form only when the coverage is over a threshold value, and they initially occupy FHUCs of the Si(111)-7×7 surface preferentially. Furthermore, by systematically analyzing the spatial distribution of Al clusters, an attractive interaction between the clusters was found, which is likely to be crucial in forming a large-scale nanocluster array with a honeycomb lattice instead of a triangular one.

II. EXPERIMENTAL DETAILS

The experiments were performed with a JEOL 4500 variable-temperature STM operated in ultrahigh vacuum (base pressure ~1×10^{-8} Pa). Samples were heated by direct electric current and the temperature was monitored by an infrared pyrometer. A chemically etched tungsten tip was used. Si(111) samples were chemically etched by HF solution ex situ and degassed at ~600 °C for several hours in situ. Then, a clean and well-ordered Si(111)-7×7 surface was obtained by flashing to ~1100 °C for several times. An electron-beam evaporator was used to deposit Al directly in the STM chamber. All STM images were recorded in situ at the growth temperature (400 °C) with constant current mode after depositing Al on the clean Si(111)-7×7 surfaces without changing the sample position.

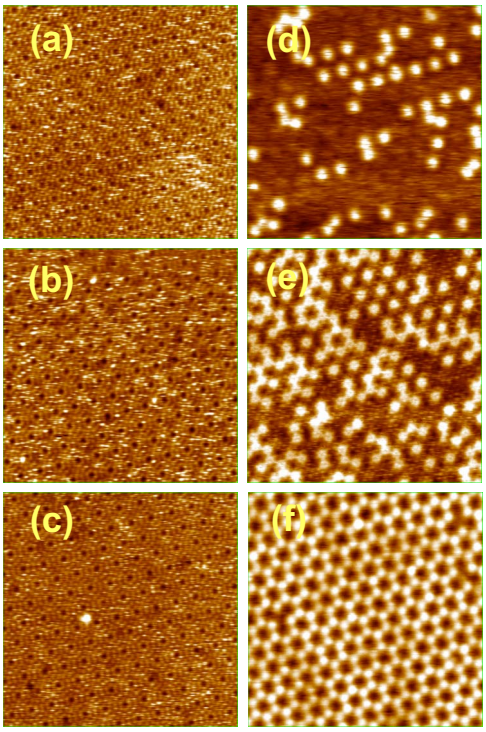

FIG. 1. (Color online) STM images of Al on Si(111)-7×7 surfaces; (a) 0.02, (b) 0.04, (c) 0.08, (d) 0.12, (e) 0.17 and (f) 0.30 ML. Scanning size: 28.6×28.6 nm^2. Sample bias: between +2.0 and 2.5 V; tunneling current: between 0.08 and 0.12 nA. Growth and observation temperature: 400 °C.

III. RESULTS AND DISCUSSIONS

Figure 1 shows STM images of Al on the Si(111)-7×7 surface with various Al depositing amounts (coverages) of (a) 0.02, (b) 0.04, (c) 0.08, (d) 0.12, (e) 0.17, and (f) 0.30 ML (1 ML=1 adsorbed atom per substrate atom), respectively, at 400 °C. When the coverage is less than ~0.08 ML, no Al clusters were observed in the scanned regions, and instead, the streaky noise appears frequently irrespective of the tip conditions.[19] The noise can be attributed to the diffusion of Al adatoms on the surface. When the coverage reaches ~0.08 ML, Al magic clusters start to be observed and, henceforth the cluster density increases with the depositing amount [Figs. 1(d)–1(f)]. At the coverage of 0.3 ML, a nearly perfect 2D Al nanocluster array with a honeycomb lattice forms, as shown in Fig. 1(f). Notably, 0.3 ML corresponds to ~14.7 at./u.c. 2.7 surplus atoms (0.06 ML) compared to the atomic structure model of the magic Al cluster.[12,13,16] The surplus Al atoms could have been depleted by initial substitution for Si adatoms (as will be discussed below), and also could diffuse too quickly on the surface of the Al nanocluster arrays at high temperature to be captured by STM observations.

Figure 2 shows the Al cluster density as a function of coverage. There is a well defined critical coverage, ~0.08±0.015 ML, beyond which Al cluster density increases linearly with the coverage. A similar (considering the uncertainty of the evaporation flux) critical coverage (0.06 ML) was also observed by Kotlyar *et al.*[13] at room temperature after growing Al nanoclusters at high temperature (560 °C). As discussed in Ref. 13, the critical coverage could be attributed to the initial Al substitution for edge and corner Si adatoms preferentially in FHUCs. Moreover, this critical behavior was found during the formation of Na magic clusters on Si(111)-7×7 even with an identical critical coverage, where the formation of a 2D adatom gas phase and a critical condensation into clusters was invoked.[14] Such a behavior might be universal for the formation of metal magic clusters on Si(111)-7×7 surfaces, though the corresponding temperature can be different from metal to metal, for example, 400 °C for Al and room temperature for Na.

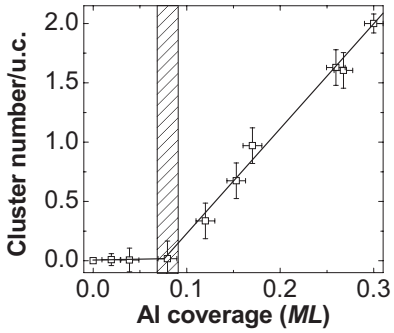

FIG. 2. Average cluster density as a function of the Al coverage.

It is evident from Fig. 1(e) that Al magic clusters do not occupy FHUCs and UHUCs equally. The STM images in the inset of Fig. 3 for 0.17 ML Al (~0.9 clusters/u.c.) indicate clearly that Al nanoclusters preferentially occupy FHUCs. This preference leads to the formation of a local triangular nanocluster lattice. Unfortunately, a long-range order of the triangular cluster lattice could not be established as yet though we have tried several deposition temperatures throughout the whole coverage range. As shown in Fig. 3, the ratio of cluster numbers between FHUCs and UHUCs

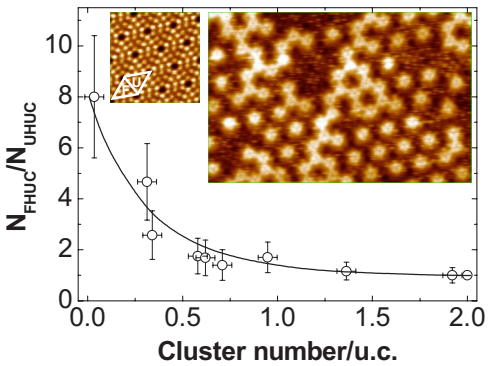

FIG. 3. (Color online) Occupation ratio between FHUCs and UHUCs as a function of the average cluster density; N_{FHUC} is the cluster number in FHUCs and N_{UHUC} the cluster number in UHUCs. The left inset shows the bare Si(111)-7×7 surface before growing Al, scanning size: 8.9×8.9 nm^2. The right inset shows a STM image 0.17 ML Al grown at 400 °C, scanning size: 26.0 ×16.8 nm^2. For both STM images, sample bias: 2.5 V; tunneling current: 0.1 nA; and imaged at 400 °C.

(N_F/N_U, N_F is the cluster number in FHUCs and N_U the cluster number in UHUCs) decreases with increasing cluster density. This behavior contrasts clearly with the case of In and Tl on Si(111),[9,12] in which nearly all clusters only occupy FHUCs initially, and suggests that, for Al, the energy difference for the cluster formation in FHUCs and UHUCs is not sufficiently large or the adatom diffusion is limited. The latter possibility is excluded since we have already observed active diffusion at low coverage and formation of low density clusters at the same temperature. Assuming that the fast diffusion implies that there is no kinetic barrier, the formation energy difference (ΔE) between the two halves of a Si(111)-7×7 unit cell can be parametrized according to the Boltzmann distribution, $N_F/N_U=\exp(-\Delta E/k_BT)$, where k_B is Boltzmann's constant and T is the temperature. For example, at 400 °C, ΔE is estimated roughly to be 0.12±0.02 eV at the initial coverage with a cluster density of 0.035 clusters/u.c. (~0.08 ML Al), which is similar to the theoretical value of 0.1 eV, calculated for the well-established structure model with *fully* periodic arrays.[12] However, ΔE decreases rapidly with increasing the Al coverage; for example, when the coverage is 0.11 ML (~0.32 clusters/u.c.), ΔE is estimated to be as small as ~0.07±0.02 eV.

The decaying preferential occupation in FHUCs with the increase of the cluster density suggests that there may be a short-range interaction between clusters. That is, an attractive interaction would result in an aggregation of Al clusters [the occupation of both FHUC and UHUC in one Si(111)-7×7 unit cell] while a repulsive interaction would result in a more uniform distribution. In order to investigate the interaction among Al nanoclusters further, we have analyzed the spatial cluster distribution carefully for various cluster densities. As an example, a STM image for a cluster density of ~0.66 clusters/u.c. (~0.15 ML Al) is shown in Fig. 4(a). Obviously, Al clusters are not uniformly distributed. More quantitatively, the distribution of Al nanoclusters on the Si(111)-7×7 substrates was characterized by a radial distribution function, as applied to systems of gas adatoms on metal substrates.[20] Considering the isolated and well defined adsorption sites on the Si(111)-7×7 surface, and also the different occupation probability of Al clusters in FHUCs (Θ_F) and UHUCs (Θ_U) as shown in Fig. 3, the two-dimensional radial distribution function at the kth nearest-neighbor site can be written as

$$g(k) = \frac{1}{N}\sum_{i=1}^{N} \frac{n_i(k)}{m(k)\,\theta_k},$$

where N is the total number of Al clusters sampled, θ_k the occupation probability of clusters at kth nearest-neighbor site ($\theta_k=\Theta_F$ when the kth nearest-neighbor site is FHUC and $\theta_k=\Theta_U$ when the kth nearest neighbor site is UHUC), $n_i(k)$ the number of kth nearest-neighbor clusters around the ith one, and $m(k)$ the number of kth nearest-neighbor sites. In fact, the radial distribution function $g(k)$ reflects the average occupation probability of the kth nearest-neighbor site normalized by the cluster coverage. For a random distribution, $g(k)$ should be 1 and independent of k (here, the unit of the cluster coverage Θ is clusters/half-unit-cell, not clusters/u.c.). In our real statistics, the $k=0$ clusters (reference clusters) were selected in FHUC and UHUC sublattices, and obtained the corresponding radical distribution function $g_F(k)$ and $g_U(k)$, respectively, where $g_F(k)/g_U(k)$ is the radial distribution function with the $k=0$ clusters in the FHUC/UHUC sublattice. The obtained $g(k)$ shown in Fig. 4(b) is an average of $g_F(k)$ and $g_U(k)$. In principle, $g_F(k)$ and $g_U(k)$ should coincide. The average is used to reduce the error. By this method, the effects of the different adsorption energy in FHUCs and UHUCs could be erased and only the interaction between clusters could be extracted. Figure 4(b) shows that $g(k)$ decreases with the distance from an existing Al cluster (especially clearly in the sample with cluster density of 0.32 clusters/u.c.) and approaches 1 when the distance is greater than 3 nm. In other words, the clusters have a larger probability to occupy those sites neighboring an existing cluster. At the nearest-neighbor site (for $k=1$, the distance is $0.58a=1.57$ nm where $a=2.7$ nm is the size of a 7×7 unit cell), for a cluster density of 0.32 and 0.66 clusters/u.c. $g(k)$ is about 2.1 and 1.2, respectively, much higher than the expected value (1.0) for random occupation. At equilibrium, the relationship between the effective interaction potential $V_{eff}(k)$, the so-called potential of mean force which describes the interaction among an ensemble of clusters, and $g(k)$ can be expressed as $g(k)=\exp[-V_{eff}(k)/k_BT]$.[20] Then, $V_{eff}(k=1)$

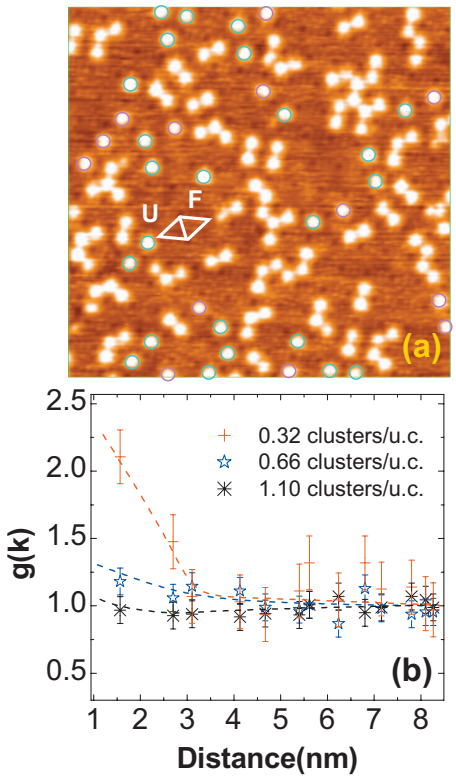

FIG. 4. (Color) (a) STM image of Al nanuclusters on the Si(111)-7×7 surface. Cluster density: ~0.66 clusters/u.c (~0.15 ML). Sample bias: 2.5 V; tunneling current: 0.08 nA. Single clusters in FHUCs/UHUCs are marked by dark cyan/magenta colors, respectively. (b) Radial distribution function $g(k)$ as a function of the distance from an existing cluster for the samples with various cluster densities. The dash lines are used as a guide for the eye.

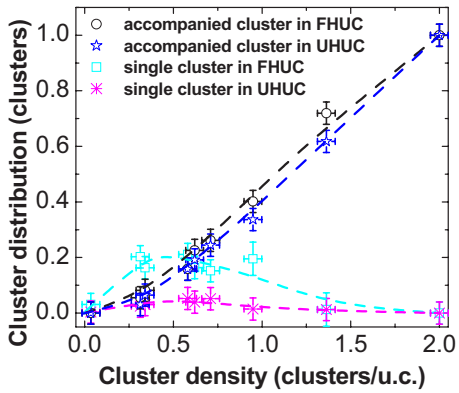

FIG. 5. (Color online) Cluster density dependence of the cluster distribution. The dash lines are used as a guide for the eye.

is estimated to be -0.04 ± 0.01 eV for a cluster density of 0.32 clusters/u.c., at the current experimental temperature (673 K), which is consistent to the decrease of the adsorption energy difference in FHUCs and UHUCs with increasing the cluster density extracted from the Boltzmann distribution.

In order to show the attractive interaction more clearly, the nearest case ($k=1$) was analyzed further. Al clusters are classified into single and accompanied clusters. The former represents those clusters occupying a unit cell alone, while the latter represents those occupying a half unit cell accompanied by at least one other cluster within the scale of one unit cell. Single clusters in FHUCs/UHUCs are marked by dark cyan/magenta colors, respectively, in Fig. 4(a). There are 24/13 single clusters and 61/52 accompanied clusters occupying FHUCs/UHUCs. That is, accompanied clusters (113) are three times more popular than single ones (37) though there are still many unoccupied unit cells. What we should emphasize is that those clusters, especially in UHUCs, prefer to share one unit cell with other clusters. These results, therefore, also indicate that a short-range attractive interaction exists among Al nanoclusters at least within a range of a unit cell.

Figure 5 shows the coverage dependence of the cluster distribution. For FHUCs, single clusters are more frequent than accompanied ones at low cluster coverage, and less frequent than accompanied ones when the cluster coverage is above ~0.3 clusters/u.c. However, for UHUCs, accompanied clusters are always more than single ones. This can be understood as follows. The cluster distribution is determined by both the formation energy difference between FHUCs and UHUCs, and the attractive intercluster interaction. The former controls the degree of preferential occupation of the FHUCs, while the latter determines the likelihood of clusters occupying both FHUCs and UHUCs within a unit cell. Due to the short-range nature of the attractive interaction among Al nanoclusters (<3 nm), when the cluster density is small, most clusters prefer to occupy FHUCs due to the lower formation energy in FHUCs. With an increase in the cluster density, the attractive interaction plays a role in the cluster distribution and accompanied clusters form instead of single clusters exclusively occupying FHUCs only. In other words, the attractive interaction among Al clusters hinders the formation of a uniform triangular cluster lattice.

The attractive interaction among Al magic clusters on Si(111)-7×7 is assumed to be an indirect, i.e., substrate-mediated interaction. The surface adsorption energy of Al adatoms can be changed due to the formation of Al nanoclusters. As with most metal atoms, Al adatoms initially prefer to occupy FHUCs on the bare Si(111)-7×7 surface due to the higher adsorption energy in FHUCs and form nanoclusters there. However, after the formation of an Al nanocluster in the FHUC, the adsorption energy in the nearest UHUCs will possibly be increased due to charge redistribution[21] or lattice strain on the surface. As a result, the next Al nanocluster will prefer to form in the UHUCs adjacent to the preformed Al nanocluster as well as in unoccupied FHUCs. Of course, not only the Al adsorption energy but also the Al cluster formation energy could be affected by the neighboring cluster within a Si(111)-7×7 unit cell. On the other hand, the substitution of Al for Si adatoms will also probably affect the distribution of the adsorption energy and even the formation energy of Al nanoclusters due to lattice distortion and charge redistribution.

Note again that, at the initial stage, In and Tl (different from In cluster, one Tl cluster consists of nine Tl atoms)[9] adatoms only occupy FHUCs and form 2D triangular lattices,[9,11] while Al and Ga were found to form preferentially honeycomb structures,[10,12] though Al, Ga, In, and Tl are isovalent. According to our results, the honeycomb structure is formed preferentially due to the attractive interaction among nanoclusters. If there is no attractive interaction, the triangular lattice should be more stable compared to the honeycomb structure considering the formation energy difference between FHUCs and UHUCs. In other words, one can speculate that the attractive interaction could exist between Al clusters as well as between Ga clusters, but not between In or Tl clusters which are larger and heavier than Al and Ga clusters. From this sense, the nearest-neighbor interaction is possibly related to atom sizes, i.e., the lattice strain effect. On the other hand, the role of the metallic surface state of Si(111)-7×7 should also be considered as in the surface-state-mediated indirect interaction of adsorbates on metal surfaces, i.e., Co or Cu adsorbates on Cu(111) surfaces.[22,23] Though the surface state of the Si(111)-7×7 will transform from metallic to insulating, as predicted by Zhang *et al.*[21] while Al nanocluster arrays form on the Si(111)-7×7, at the initial stage of forming Al clusters, the Si(111)-7×7 surface was covered partially by Al clusters and metallic feature of the bare Si(111)-7×7 should not be changed even near the existing Al nanoclusters. Considering the localized nature of the surface electrons (from dangling bonds) and the observed short force range [around a unit cell of Si(111)-7×7)], as an analog of the surface-state-mediated indirect interaction of adsorbates on metal surfaces, the electron-mediated mechanism could not be excluded. The exact microscopic mechanism of the intercluster interaction cannot be pinned down at present and a further theoretical study is highly required.

IV. SUMMARY

In summary, we report a study on the formation process of Al nanocluster arrays on the Si(111)-7×7 surface at high

temperature by means of high temperature STM imaging. It was found that Al magic clusters form only when the Al coverage is beyond a critical value. The clusters initially occupy the FHUCs preferentially but the preference decays with increasing Al coverage. Moreover, an attractive interaction among clusters was found by analyzing the cluster distribution systematically and possible mechanism is discussed.

ACKNOWLEDGMENTS

The authors thank Yagi for help in sample preparation and K. H. Wu for constructive discussion. The authors acknowledge the financial support from MEXT, Japan. H.W.Y. is supported through CAWL of the CRi Program of MOST, Korea and is grateful for the financial support from ICYS of NIMS.

*Author to whom correspondence should be addressed; FAX: 81-29-860-4706; runwei.li@nims.go.jp

[1] J. V. Barth, G. Costantini, and K. Kern, Nature (London) **437**, 671 (2005).
[2] F. Rosei, J. Phys.: Condens. Matter **16**, S1373 (2004).
[3] P. Moriarty, Rep. Prog. Phys. **64**, 297 (1998).
[4] M. Valden, X. Lai, and D. W. Goodman, Science **281**, 1647 (1998).
[5] A. O. Orlov, I. Amlani, G. H. Bernstern, C. S. Lent, and G. L. Snider, Science **277**, 928 (1997).
[6] S. Sun, C. B. Murray, D. Weller, L. Folks, and A. Moser, Science **287**, 1989 (2000).
[7] T. Koide, H. Miyauchi, J. Okamoto, T. Shidara, A. Fujimori, H. Fukutani, K. Amemiya, H. Takeshita, S. Yuasa, T. Katayama, and Y. Suzuki, Phys. Rev. Lett. **87**, 257201 (2001).
[8] H. Brune, M. Giovannini, K. Bromann, and K. Kern, Nature (London) **394**, 451 (1998).
[9] L. Vitali, M. G. Ramsey, and F. P. Netzer, Phys. Rev. Lett. **83**, 316 (1999).
[10] M. Y. Lai and Y. L. Wang, Phys. Rev. B **64**, 241404(R) (2001).
[11] J. L. Li, J. F. Jia, X. J. Liang, X. Liu, J. Z. Wang, Q. K. Xue, Z. Q. Li, J. S. Tse, Z. Y. Zhang, and S. B. Zhang, Phys. Rev. Lett. **88**, 066101 (2002).
[12] J. F. Jia, J. Z. Wang, X. Liu, Q. K. Xue, Z. Q. Li, Y. Kawazoe, and S. B. Zhang, Appl. Phys. Lett. **80**, 3186 (2002); J. F. Jia, X. Liu, J. Z. Wang, J. L. Li, X. S. Wang, Q. K. Xue, Z. Q. Li, Z. Zhang, and S. B. Zhang, Phys. Rev. B, **66**, 165412 (2002).
[13] V. G. Kotlyar, A. V. Zotov, A. A. Saranin, T. V. Kasyanova, M. A. Cherevik, I. V. Pisarenko, and V. G. Lifshits, Phys. Rev. B **66**, 165401 (2002).
[14] K. Wu, Y. Fujikawa, T. Nagao, Y. Hasegawa, K. S. Nakayama, Q. K. Xue, E. G. Wang, T. Briere, V. Kumar, Y. Kawazoe, S. B. Zhang, and T. Sakurai, Phys. Rev. Lett. **91**, 126101 (2003).
[15] S. C. Li, J. F. Jia, R. F. Dou, Q. K. Xue, I. G. Batyrev, and S. B. Zhang, Phys. Rev. Lett. **93**, 116103 (2004).
[16] H. H. Chang, M. Y. Lai, J. H. Wei, C. M. Wei, and Y. L. Wang, Phys. Rev. Lett. **92**, 066103 (2004).
[17] Run-Wei Li, S. Kusano, J. H. G. Owen, and K. Miki, Nanotechnology **17**, 2018 (2006).
[18] Run-Wei Li, S. Kusano, J. H. G. Owen, and K. Miki, Appl. Phys. Lett. **89**, 073116 (2006).
[19] Before the *Al* deposition, we can obtain very clear *STM* images of Si(111)-7×7 surface easily under this condition, as shown in the left inset of Fig. 3.
[20] J. Trost, T. Zambelli, J. Wintterlin, and G. Ertl, Phys. Rev. B **54**, 17850 (1996).
[21] L. Zhang, S. Zhang, Q. Xue, J. Jia, and E. Wang, Phys. Rev. B **72**, 033315 (2005).
[22] J. Repp, F. Moresco, G. Meyer, K. H. Rieder, P. Hyldgaard, and M. Persson, Phys. Rev. Lett. **85**, 2981 (2000).
[23] N. Knorr, H. Brune, M. Epple, A. Hirstein, M. A. Schneider, and K. Kern, Phys. Rev. B **65**, 115420 (2002).